

Effects of polycaprolactone/hydroxyapatite nanocomposite scaffolds combined with platelet-rich fibrin for repair of rabbit calvarial bone defects

Sina Yal Beiranvand¹, Shiva Amanollahi², Hossein Nourani³, Hossein Kazemi Mehrjerdi^{1*}

¹ Department of Clinical Sciences, Faculty of Veterinary Medicine, Ferdowsi University of Mashhad, Mashhad, Iran; ² Department of Clinical Sciences, School of Veterinary Medicine, Shiraz University, Shiraz, Iran; ³ Department of Pathobiology, Faculty of Veterinary Medicine, Ferdowsi University of Mashhad, Mashhad, Iran.

Article Info

Article history:

Received: 09 May 2025

Accepted: 19 July 2025

Available online: 15 April 2026

Keywords:

Bone defect repair
Hydroxyapatite
Platelet-rich fibrin
Polycaprolactone
Scaffold

Abstract

Bone tissue engineering offers a potential alternative to conventional grafting by combining biocompatible scaffolds with biological stimulants. Polycaprolactone (PCL) is a biodegradable polyester with good mechanical strength and biocompatibility. Hydroxyapatite (HA) is a calcium phosphate mineral that is a major component of bone and has excellent bioactivity and biocompatibility. This research investigated the histopathological effects of PCL-HA nanocomposite scaffolds along with their combination with platelet-rich fibrin (PRF), on the regeneration of bone in rabbit calvarial bone defects. Four circular full-thickness bone defects of 5.00 mm in diameter were created on the calvarial bone of 15 male New Zealand white rabbits. Three defects were filled with PRF, PCL-HA, and PCL-HA/PRF, and one defect was served as a control with no filler. Histopathological evaluations were conducted at 4-, 8-, and 12-weeks post-implantation. Data were evaluated using the Kruskal-Wallis and Mann-Whitney U tests. Significant differences were observed between the treatment and control groups regarding bone regeneration throughout all 12th weeks studied. In the 4th weeks, no significant differences in bone regeneration were noted among the treatment groups. In the 8th weeks, most new bone formation was observed in the PCL-HA/PRF group. Both the PCL-HA and PCL-HA/PRF groups significantly improved bone regeneration compared to the control and PRF groups, with the PCL-HA/PRF group demonstrating the greatest bone formation, and vascularization and the lowest inflammation by the 12th week. Thus, PCL-HA/PRF could be considered as a suitable alternative to bone grafts and could be increasingly utilized in orthopedic surgery and bone tissue engineering.

© 2026 Urmia University. All rights reserved.

Introduction

Bone tissue is one of the most important components that play multiple roles in daily life.¹ Many patients suffer from bone disease resulting from tumor removal, trauma, infection, cysts, and accidental injuries.² Bone graft transplantation (autogenous, allogeneic, or xenogeneic) and artificial bone implants are used to treat these conditions.³ The primary traditional option for patients with bone defects is autogenous bone transplantation.^{4,5} However, complications and secondary injuries are potential risks associated with tissue grafts.^{6,7} Today, bone tissue engineering, a suitable substitute for bone grafts, has no mentioned complications. Combining biodegradable and porous scaffolds with signaling factors may provide appropriate cell adhesion, proliferation, function, tissue restoration and vascularization.⁸ Due to the complex factors involved in creating these materials,

achieving an ideal combination is challenging. More studies are needed for the effective therapeutic application of this intriguing, promising and complex technology.⁹

One of the most common materials used for fabricating scaffolds for bone tissue regeneration is polycaprolactone (PCL). The PCL exhibits good biocompatibility and a slow degradation rate compared to other polyesters, and generates less acidic breakdown products and demonstrates potential for load-bearing applications.^{10,11} Since bone requires time to remodel and regenerate, the slow degradation of PCL facilitates this process and can also be adjusted to modify the polymer biodegradation rates.^{12,13} Additionally, due to its melting temperature of 55.00 - 60.00 °C, it is one of the most preferred polymers for extrusion-based three-dimensional (3D) printing.¹² Studies have shown that PCL has good mechanical properties, exhibiting high flexibility and great elongation when preparing scaffolds for craniofacial bone repair.¹⁴

*Correspondence:

Hossein Kazemi Mehrjerdi. DVM, DVSc

Department of Clinical Sciences, Faculty of Veterinary Medicine, Ferdowsi University of Mashhad, Mashhad, Iran

E-mail: h-kazemi@um.ac.ir



This work is licensed under a Creative Commons Attribution-NonCommercial-ShareAlike 4.0 International (CC BY-NC-SA 4.0) which allows users to read, copy, distribute and make derivative works for non-commercial purposes from the material, as long as the author of the original work is cited properly.

However, pure PCL has no osteogenic potential to induce bone regeneration.¹⁵ Therefore, researchers have demonstrated that the combination of PCL with various polyesters, inorganic substances, metal elements or collagen enhances the properties of the scaffolds.¹⁶

Hydroxyapatite (HA) is composed of calcium and phosphates. It can be found naturally in biological sources such as mammalian bones, marine sources, shells, plants, algae and minerals such as limestone.¹⁷ The HA can also be chemically synthesized in different shapes and particle sizes.¹⁸ It can be combined with many natural, synthetic polymers or growth factors/cells to mimic the natural structure of bone to achieve bone formation and remodeled by increasing its osteoconductivity, osteo-inductivity or both.¹⁹

Platelet-rich fibrin (PRF) is an autologous derived bioactive material that consists of a fibrin scaffold, growth factors, platelets and leukocytes. It releases the physiological doses of growth factors slowly and gradually degrades the fibrin scaffold.²⁰⁻²² The PRF promotes vascular regeneration, proliferation and migration of osteoblast-related cells (mesenchymal cells, osteoblasts, and osteoclasts) while having certain immunomodulatory and anti-bacterial effects. As a result, it has excellent osteogenic potential and is used in bone tissue engineering. For the improvement of its biological properties, it is often combined with bone tissue engineering scaffolds to enhance its mechanical properties and delay degradation.²³

This study represented the first *in vivo* investigation that integrated 3D-printed PCL-HA nanocomposite scaffolds with PRF for repairing calvarial bone defects in rabbits. Although we previously demonstrated the cytocompatibility and osteogenic potential of PCL-HA/PRF scaffolds *in vitro*, this study provided the first *in vivo* histopathological evidence supporting their superior performance in bone regeneration over PCL-HA or PRF alone. Considering the limitations of using bone autografts and allografts, the results of this study provided valuable information about the use of tissue engineering in bone defects (extensive defects) and non-union as a suitable alternative to bone grafting.

Materials and Methods

Scaffold Preparation. The scaffolds were fabricated using 3D printing technology (Omid Afarinan, Tehran, Iran) to provide a suitable environment for bone regeneration. Scanning electron microscopy (MIRA3; Tescan, Brno, Czech Republic), Fourier transform infrared and compression tests were used to characterize the scaffold morphology, microstructure and mechanical properties. A previous study also investigated the potential for cell adhesion, proliferation, biocompatibility and differentiation. The 3D PCL-HA scaffold with linked pores

had a moderately rough surface due to HA nanoparticle incorporation which increased mechanical properties. Increased bone cell proliferation on the PCL-HA/PRF scaffold surface was seen as a result of the enhanced hydrophilicity and porosity of the PCL-HA/PRF scaffold compared to the PCL scaffold. The 3-(4,5-dimethylthiazol-2-yl)-2,5-diphenyl-2H-tetrazolium bromide (MTT) assay results has shown that the PCL-HA/PRF scaffold was much more cytocompatible than the PCL and PCL-HA scaffolds, which was a major improvement.²⁴

Animal modeling. This study randomized 15 healthy 1-year-old New Zealand male rabbits (weight ~2.50 kg) into three groups. Two weeks before the surgery, the rabbits were placed in separate cages with free access to water and pelleted food (Javaneh Khorasan, Mashhad, Iran), under 12-hr cycles of light and darkness and proper ventilation and temperature (22.00 - 26.00 °C). The bedding was changed daily. Rabbits were anesthetized by intramuscular injection of 40.00 mg kg⁻¹ ketamine (Bremer Pharma GmbH, Warburg, Germany) and 4.00 mg kg⁻¹ xylazine (Alfasan, Woerden, The Netherlands).²⁵ The PRF was extracted from 3.00 mL of peripheral blood of each rabbit according to the protocol.²⁶ The scaffolds were cut in dimensions of 5.00 × 5.00 mm and sterilized with 25.00 kGy gamma rays for 10 hr. The rabbit calvarial bone defect was created according to the previous study.^{27,28} The back area of the calvarium bone was prepared aseptically for surgery. Following a midline skin incision (40.00 mm), the muscle was dissected and the periosteum was elevated to reveal the calvarial bone carefully. Four full-thickness circular defects, each measuring 5.00 mm in diameter were created in the skull using a high-speed burr (NE 116; NSK-Nakanishi, Kanuma, Japan) while continuously irrigating with sterile saline. The surgical procedure was performed with appropriate caution to reduce any damage to the dura mater. Three defects were filled randomly with PRF, PCL-HA, and PCL-HA/PRF. One defect was left untreated as a control. In the other rabbits, the location of the groups in the created cavities was rotated clockwise and recorded. Finally, the periosteum using Vicryl 4-0 (Supa, Tehran, Iran), subcutaneous tissue using Vicryl 3-0 (Supa), and skin using Nylon 3-0, (Supa) were sutured (Fig. 1). Post-operative care included the subcutaneous administration of 5.00 mL Ringer's solution (Iran Injectable and Pharmaceutical Products Co., Tehran, Iran), injections of enrofloxacin (10.00 mg kg⁻¹, Subcutaneous, q12hr, 5 days; Razak, Tehran, Iran) and tramadol (5.00 mg kg⁻¹, Subcutaneous, q12hr, 3 days; Darou Pakhsh pharmaceutical Co., Tehran, Iran). The skin sutures were removed 14 days after surgery. The study was conducted with the approval of the Research Ethics Committee of Ferdowsi University of Mashhad (IR.UM.REC.1401.023). All experimental procedures were implemented according to the ethical guidelines for studying experimental pain in conscious animals.



Fig. 1. Experiment design. A view of the defects created on rabbit calvarium bone and the locations of different groups. PRF: Platelet-rich fibrin; HA: Hydroxyapatite; PCL: Polycaprolactone.

Histopathology evaluation. At 4, 8, and 12 weeks after bone defect creation, rabbits were euthanized by intravenous 100 mg kg⁻¹ sodium thiopental (Loghman, Tehran, Iran) for histopathology evaluation. The bone was harvested *en bloc* encompassing four defects. For histopathological studies, the calvarium bone of rabbits was fixed with 10.00% formalin for 48 hr. Then, all the samples were decalcified in a 5.00% hydrochloric acid solution for 72 hr. The decalcified samples were washed with phosphate-buffered saline and then prepared using the standard paraffin embedding method. The obtained paraffin blocks were divided by microtome into slices with a thickness of 5.00 μ m and transferred onto a glass slide. Finally, the samples were stained with Hematoxylin and Eosin for histological examination. The specimens were evaluated under a light microscope.²⁹ A blinded observer performed the histopathological assessment. For a semi-quantitative histological evaluation, histopathological images were scored on a scale of one to 10 based on the amount of new bone formed, quality of bone (woven vs. lamellar), vascularization and the presence or lack of inflammation, summarized in Table 1.³⁰ Also, a modified grading system based on Emery *et al.* method was applied as follows: Grade 0: when the gap was empty, Grade 1: Where the gap was filled with fibrous connective tissue only, Grade 2: Where the gap was filled with fibrous tissue more than fibrous-immature bone tissue, Grade 3: Where

fibrous-bone tissue was more than fibrous tissue, Grade 4: Where the gap was covered with fibrous-immature bone, Grade 5: Fibrous-immature bone was more than mature bone, Grade 6: Mature bone was more than fibrous-immature bone tissue and Grade 7: Where the gap was only completed with mature bone.³¹

Statistical analysis. All data were reported as the median (Q1 - Q3) and SPSS Software (version 26.0; IBM Corp., Armonk, USA) was used for the analysis. The histological results among various groups were analyzed statistically using the non-parametric Kruskal-Wallis test. When *p* values were found to be less than 0.05, pairwise comparisons between groups were carried out using the Mann-Whitney U test. The graphs are drawn using GraphPad Prism (version 9.5; GraphPad Software Inc., San Diego, USA).

Results

Histopathological evaluations. In the histopathology evaluation at the 4th week post-surgery, the defect was filled with blood clots and connective tissue bridged in the control group. Connective tissue bridged and mild fibrous-woven bone formation were seen in the defects filled with PRF. While in the groups of PCL-HA and PCL-HA/PRF, the defects were filled with fibrous-woven bone and mild mature bone formation. Neither foreign body reaction nor inflammatory response was visible in the PRF and PCL-HA groups. Mild infiltration of inflammatory cells was detected in the control (1 : 5) and PCL-HA/PRF (2 : 5) groups (Fig. 2).

Statistical analysis of histopathology results in 4th week showed that the control group had the lowest bone defect coverage and new bone formation than the other groups. Also, bone defect coverage in the PCL-HA group was higher than in the PRF group (*p* < 0.05), and between the control and PRF groups was not significant (*p* > 0.05). In terms of vascularization and inflammation, no significant differences were seen among the groups. The Emery score evaluation showed that the result was lower in the control group than in the other groups, and in the PRF group was lower than the PCL-HA group (Fig. 3).

Table 1. The histological scoring system used to grade bone healing.²⁸

Scores	Bone defect coverage ^a	New bone type ^b	Vascularization ^c	Inflammation ^d
0	0.00%	No new bone	No evidence of neovascularization	Abundant inflammation and evidence of encapsulation
1	1.00 - 24.00%	Predominantly woven	Few new vessels (<10)	Relatively few (10 - 50) inflammatory cells present
2	25.00 - 49.00%	Predominantly lamella remodeled	Abundant neovascularization	No evidence of inflammatory cell presence
3	50.00 - 74.00%	-	-	-
4	75.00 - 100%	-	-	-

^a Percentage of defect bridged by bone, ^b Nature of the new bone within the defect, ^c Presence of vascularization within newly formed bone, and ^d The presence of inflammatory cells around the newly formed bone.

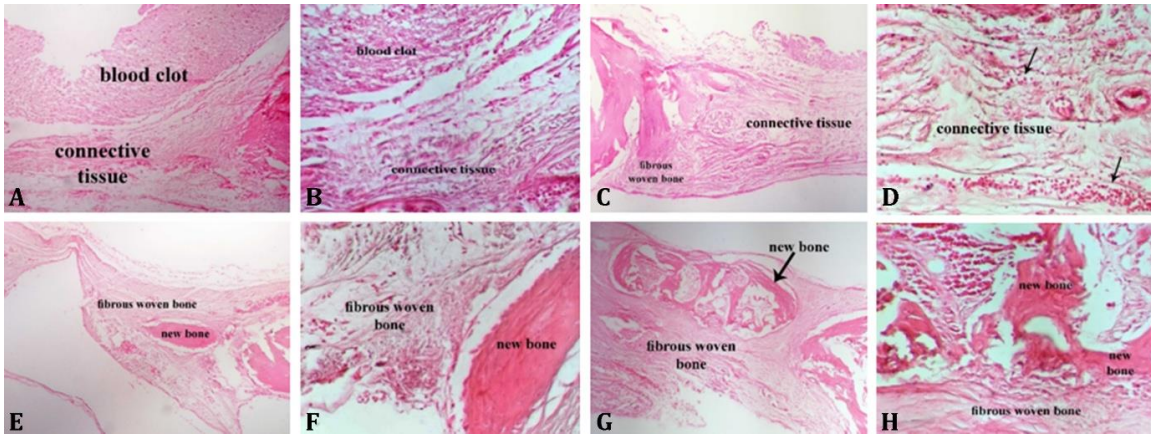


Fig. 2. Hematoxylin - Eosin staining of tissue samples of control, platelet-rich fibrin (PRF), polycaprolactone (PCL) - hydroxyapatite (HA) and PCL-HA/PRF groups in the 4th week of post-surgery. **A, B)** Connective tissue bridges in the control group. **C, D)** Connective tissue bridges and mild fibrous-woven bone formation in the PRF group. **E-H)** Fibrous-woven bone formation and mild mature bone formation in the PCL-HA and PCL-HA/PRF groups (A - D: 100 × and E - H: 400 ×).

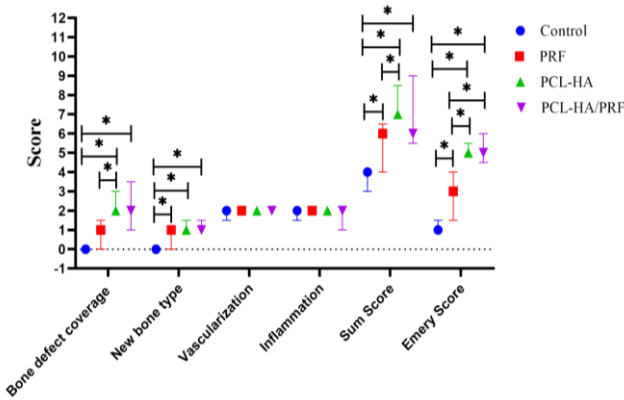


Fig. 3. Microscopic semi-quantitative results between different groups after the 4th weeks. * Denotes a significant difference between groups ($p < 0.05$; $n = 5$). All data were reported as the median and analyzed with the Kruskal-Wallis test and Mann - Whitney U tests. PRF: Platelet-rich fibrin; HA: Hydroxyapatite; PCL: Polycaprolactone.

At the end of the 8th weeks, connective tissue was bridged and fibrous-woven bone bridges were seen, respectively, in the defects of the control and PRF groups. Also, the defects of the PCL-HA group were filled with fibrous-woven bone bridges. However, a mature bony bridge was seen in the defects filled with PCL-HA/PRF. Neither foreign body reaction nor inflammatory response was visible in the PRF and PCL-HA groups. Mild infiltration of inflammatory cells was seen in the control (3 : 5) and PCL-HA/PRF (1 : 5) groups (Fig. 4).

Statistical analysis of histopathology results in 8th weeks showed that bone defect coverage was significantly higher in the PCL-HA/PRF group than in the control group. Regarding new bone formation, the PCL-HA/PRF group was higher than the other groups ($p < 0.05$). The amount of vascularization in the control group was significantly lower than in the other groups ($p < 0.05$). Generally, the total score result was lower in the control group than in the other groups. Also, in Emery's score, the PCL-HA/PRF group was higher than the control and PRF groups (Fig. 5).

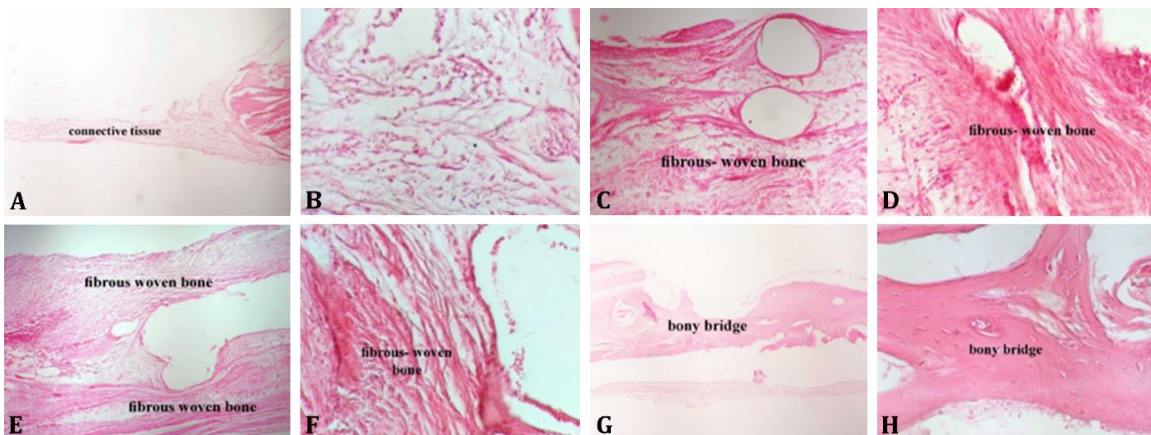


Fig. 4. Hematoxylin-Eosin staining of tissue samples of control, platelet-rich fibrin (PRF), polycaprolactone (PCL) - hydroxyapatite (HA) and PCL-HA/PRF groups in the 8th week of post-surgery. **A, B)** Connective tissue bridges in the control group. **C, D)** Fibrous-woven bone bridges in the PRF group. **E, F)** Fibrous-woven bone bridges in the PCL-HA group. **G, H)** Mature bony bridge in the PCL-HA/PRF group (A - D: 100 × and E - H: 400 ×).

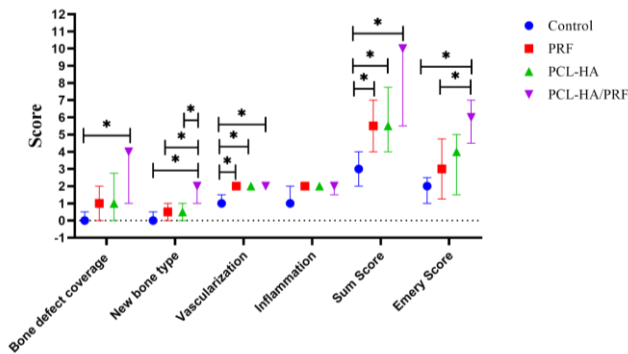


Fig. 5. Microscopic semi-quantitative results between different groups in the 8th weeks. * Denotes a significant difference between groups ($p < 0.05$; $n = 5$). All data were reported as the median and analyzed with the Kruskal-Wallis and Mann-Whitney U tests. PRF: Platelet-rich fibrin; HA: Hydroxyapatite; PCL: Polycaprolactone.

At the end of the 12th weeks, connective tissue was bridged and mild fibrous-woven bone formation was seen in the control and PRF groups, respectively. The fibrous-woven bone bridge with mild mature bone formation was seen in the defects filled with PCL-HA. Also, a mature bone bridge was seen in the defects filled with PCL-HA/PRF. In the control (4 : 5), PRF (2 : 5) and PCL-HA groups mild infiltration of inflammatory cells were detected. Neither foreign body reaction nor inflammatory response was visible in the PCL-HA/PRF group (Fig. 6).

Statistical analysis of histopathology results at the end of the 12th weeks showed that the bone defect coverage and new bone formation were higher in the PCL-HA/PRF group than in the other groups. The amount of vascularization in the PCL-HA/PRF group was higher than in control group. Generally, the total score results in the PCL-HA/PRF group were greater than those in control and PRF groups ($p < 0.05$), and the PCL-HA group exhibited

a significant difference compared to the control group. Additionally, in the Emery score results, the PCL-HA/PRF and PCL-HA groups demonstrated a substantial difference from the control and PRF groups ($p < 0.05$; Fig. 7).

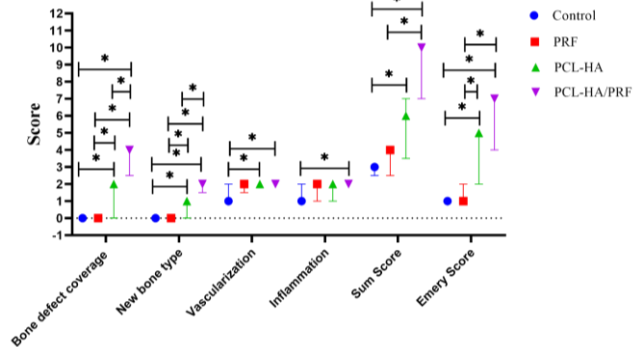


Fig. 7. Microscopic semi-quantitative results between different groups after the 12th weeks. * Denotes a significant difference between groups ($p < 0.05$; $n = 5$). All data were reported as the median and analyzed with the Kruskal-Wallis and Mann-Whitney U tests. PRF: Platelet-rich fibrin; HA: Hydroxyapatite; PCL: Polycaprolactone.

Discussion

Today, accelerating the healing process of fractures is crucial because it increases the speed of recovery, thereby reducing movement limitations and problems during the recovery period for the patient.³² Bone repair involves the formation of tissues such as fibrous connective tissue, cartilage and fibrous-woven bone that precede final bone repair.³³ In a previous study, we compared the physicochemical characteristics of the PCL, PCL-HA and PCL-HA/PRF scaffolds, and the survival rate and proliferation of osteoblast cells on these scaffolds were investigated. Cytocompatible properties and osteogenic differentiation capability *in vitro* of PCL-HA/PRF scaffolds were shown previously.²⁴ This advantage enhances bone

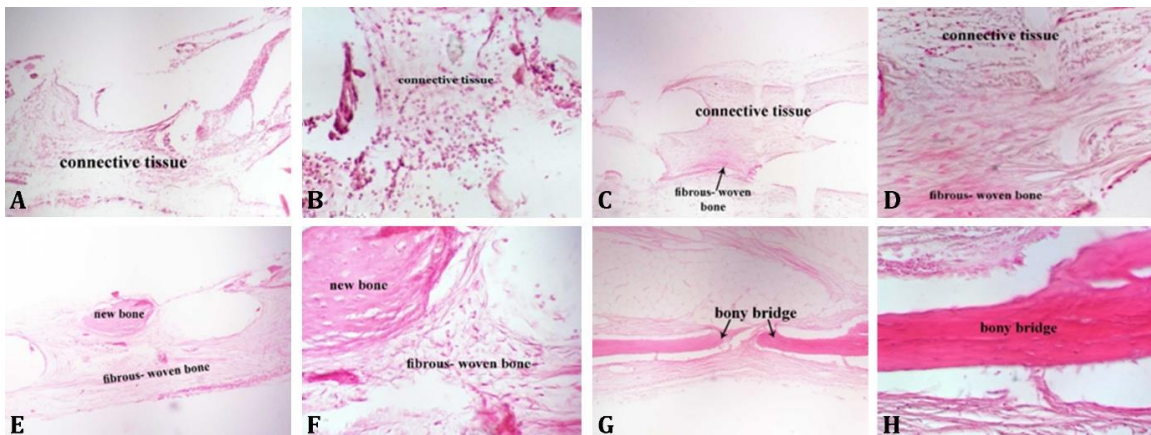


Fig. 6. Hematoxylin-Eosin staining of tissue samples of control, platelet-rich fibrin (PRF), polycaprolactone (PCL), hydroxyapatite (HA) and PCL-HA/PRF groups in the 12th week of post-surgery. **A, B)** Connective tissue bridges in the control group. **C, D)** Connective tissue bridges with mild fibrous-woven bone formation in the PRF group. **E, F)** fibrous-woven bone bridge with mild mature bone formation in the PCL-HA group. **G, H)** Mature bony bridge in the PCL-HA/PRF group (A - D: 100 × and E - H: 400 ×).

regeneration and reduces or prevents the risk of rejection complications in reparative bone formation. The biomaterial provides mechanical support and osteoconductivity for the engineered bone graft scaffold. The PCL and HA are not cytotoxic and are routinely used in clinical situations. Also, the positive effects of PCL-HA composites on osteoblasts have been demonstrated.^{34,35} According to the outstanding features of the 3D-printed PCL-HA, we investigated it *in vivo*.

In this study, the rabbit calvarial bone defect model was employed because it is a suitable preclinical research method for evaluating the efficacy of biomaterials before their veterinary and human applications.³⁶ Research has indicated that the critical size of cranial defects in rabbits for implantation durations of up to 24th weeks is 15.00 mm.³⁷ Based on previously established protocols in calvarial defect models, this study used non-critical size defects of 5.00 mm instead of critical size defects. This size enables standardized and reproducible assessment of bone regeneration.²⁷ Additionally, using four defects *per* animal helped us to test multiple treatment conditions (control, PRF, PCL-HA, and PCL-HA/PRF) within the same biological environment, reducing inter-animal variability and aligning with ethical principles by minimizing the number of animals required.

Hwan Jung *et al.*, investigated the effect of autogenous tooth biomaterial (HA and calcium phosphate minerals) combined with PRF (derived from the ear blood of rabbits) and PRF alone on monocortical defects created on each tibia of New Zealand white rabbits. Similar to the present study, they showed that after 8 weeks, tooth biomaterial enriched with PRF and tooth biomaterial alone showed more enhanced regeneration than PRF alone. Also, there was no considerable difference between the PRF and unfilled control groups. They stated that the reason may be partially due to difficulty in retention of PRF at the defect site because of the anatomy of the tibia, and an appropriate scaffold is required to successfully form new bone.³⁸⁻⁴⁰ Contrary to these studies, Lee *et al.*, showed that peri-implant defects in the tibia were successfully repaired by the application of PRF alone in comparison with the control group.⁴¹ In another study, the potential of tooth biomaterials mixed with PRF *in vivo* as bone graft materials in bone formation of round-shaped defects in the skull of New Zealand white rabbits was assessed. Similar to the present study, the histomorphometry results between all groups showed that the average amount of new bone formation was statistically higher in the tooth biomaterial+PRF group, and in the control and PRF groups was lower than in other groups. Also, the computerized tomography (micro-CT) result showed that the difference between the PRF group and the unfilled control group was not statistically significant. So, tooth biomaterial was used as a bone graft material with PRF to promote the restoration of bony defects.⁴² It has been reported that

when using PRF without bone graft material, bone formation fails and inhibits healing.⁴³ Also, in another study, a 900 mm pore-sized 3D printed PCL scaffold with PRF was implanted in a critical-sized calvaria defect of the rat without adding any bone graft or membrane. They showed that when a 3D-printed PCL scaffold was used, the bone tissues grew into the central zone of the critical defect. In contrast, the new bones were formed mostly along the margins of the defect, and the central zones of the defects collapsed and healed with thin connective tissue in the groups without the scaffolds. They stated that the concentrations of growth factors and the allogenic origins in the PRF might not achieve effectiveness. Also, to prevent soft tissue from invading during the early healing period, a barrier is needed to obtain a better outcome.⁴⁴ Comparing the PCL-HA group with the PCL-HA/PRF group showed a significant increase in bone formation after the 8th and 12th weeks in the PCL-HA/PRF group. Other studies showed that PRF is an autologous product that reduces infections and immunologic reactions.⁴⁵ The alpha granule of the platelet releases growth factors, including transforming growth factor, platelet-derived growth factor, vascular endothelial growth factor, epidermal growth factor and insulin-like growth factor-1. These growth factors play a fundamental role in the initial healing mechanism.^{42,44} The amount of vascularization in the PCL-HA/PRF, PCL-HA and PRF groups was higher than in the control group in last 8 weeks. Vascular development always precedes osteogenesis. As the vascular network is well-developed, the osteoblasts produce osteoid, then calcify and differentiate into osteocytes and finally, healthy bone is formed.⁴⁶ The application of tissue-engineered bone with a vascular network that temporally precedes the new bone formation and spatially originates from within the scaffolds is critical.⁴⁷ The presence of vascular endothelial growth factor in PRF and HA-containing polymers causes cell anchorage and growth to a certain extent. HA can absorb several important extracellular matrix proteins.⁴⁸⁻⁵⁰

The promising *in vivo* performance of our PCL-HA/PRF scaffold suggested several potential clinical applications, including repair of craniofacial defects (e.g., after tumor resection or congenital deformity correction), augmentation of alveolar ridges in dental implantology and non-load-bearing orthopedic reconstructions such as small long-bone or pelvic defects. Because the scaffold is 3D-printable, patient-specific geometries could be fabricated to match complex defect anatomies and incorporation of autologous PRF minimizes the risk of immune reactions while delivering endogenous growth factors. However, several translational hurdles remain. First, scale-up from a rabbit calvarial model to larger human defects will require validation of mechanical properties under physiologic loads and optimization of scaffold porosity for ingrowth and vascularization. Second,

manufacturing reproducibility, sterilization logistics (to ensure consistent 25.00 kilogray dosing without degrading PRF bioactivity), and regulatory approval pathways for combination products (device plus biologic) must be navigated. Third, long-term safety and efficacy data—including monitoring for late-stage resorption, remodeling, and potential inflammatory responses—are needed in large-animal models before initiating clinical trials. Addressing these challenges through iterative preclinical studies and early-phase human feasibility trials will be critical for bringing this technology to patient care.

This study had several limitations that should be acknowledged. First, the sample size was relatively small (five animals per time point), which might have limited the statistical power and the generalizability of the results. Second, although the rabbit calvarial defect model is widely accepted for evaluating bone regeneration due to its reproducibility and relevance, it does not fully replicate the complexity of human bone healing, particularly in load-bearing areas. Third, the follow-up period was limited to 12 weeks, which might not have been sufficient to assess the regenerated bone long-term stability, remodeling and integration. Future studies with larger sample sizes, additional animal models and extended observation periods are recommended to confirm and expand upon these findings.

In conclusion, the results of the present study demonstrated that a logical combination containing the required components such as a biocompatible biomaterial scaffold and specific cells responsible for vascularization and osteogenesis offered a promising strategy for engineered bone healing.

Acknowledgments

The authors thank the staff of the Faculty of Veterinary Medicine Teaching Hospital of Ferdowsi University of Mashhad, Mashhad, Iran for their technical cooperation.

Conflict of interest

The authors declare no conflict of interest.

References

- Bhattacharjee P, Kundu B, Naskar D, et al. Silk scaffolds in bone tissue engineering: an overview. *Acta Biomater* 2017; 63: 1-17.
- Samorezov JE, Alsberg E. Spatial regulation of controlled bioactive factor delivery for bone tissue engineering. *Adv Drug Deliv Rev* 2015; 84: 45-67.
- Shang F, Yu Y, Liu S, et al. Advancing application of mesenchymal stem cell-based bone tissue regeneration. *Bioact Mater* 2021; 6(3): 666-683.
- Bishop ES, Mostafa S, Pakvasa M, et al. 3-D bioprinting technologies in tissue engineering and regenerative medicine: current and future trends. *Genes Dis* 2017; 4(4): 185-195.
- Derakhshanfar S, Mbeleck R, Xu K, et al. 3D bioprinting for biomedical devices and tissue engineering: a review of recent trends and advances. *Bioact Mater* 2018; 3(2): 144-156.
- Yan Q, Dong H, Su J, et al. A review of 3D printing technology for medical applications. *Engineering* 2018; 4(5): 729-742.
- Huang KH, Wang CY, Chen CY, et al. Incorporation of calcium sulfate dihydrate into a mesoporous calcium silicate/poly- ϵ -caprolactone scaffold to regulate the release of bone morphogenetic protein-2 and accelerate bone regeneration. *Biomedicines* 2021; 9(2): 128. doi: 10.3390/biomedicines9020128.
- Rohman G, Langueh C, Ramtani S, et al. The use of platelet-rich plasma to promote cell recruitment into low-molecular-weight fucoidan-functionalized poly (ester-urea-urethane) scaffolds for soft-tissue engineering. *Polymers (Basel)* 2019; 11(6): 1016. doi: 10.3390/polym11061016.
- DeCamp CE, Johnston SA, Déjardin LM, et al. Brinker, Piermattei and Flo's Handbook of small animal orthopedics and fracture repair. 5th ed. St. Louis, USA: Elsevier Saunders 2015; 29-32.
- Lee H, Yeo M, Ahn S, et al. Designed hybrid scaffolds consisting of polycaprolactone microstrands and electrospun collagen-nanofibers for bone tissue regeneration. *J Biomed Mater Res B Appl Biomater* 2011; 97(2): 263-270.
- Zimmerling A, Yazdanpanah Z, Cooper DML, et al. 3D printing PCL/nHA bone scaffolds: exploring the influence of material synthesis techniques. *Biomater Res* 2021; 25(1): 3. doi: 10.1186/s40824-021-00204-y.
- Seyedsalehi A, Daneshmandi L, Barajaa M, et al. Fabrication and characterization of mechanically competent 3D printed polycaprolactone-reduced graphene oxide scaffolds. *Sci Rep* 2020; 10(1): 22210. doi: 10.1038/s41598-020-78977-w.
- Cakmak AM, Unal S, Sahin A, et al. 3D printed polycaprolactone/gelatin/bacterial cellulose/hydroxyapatite composite scaffold for bone tissue engineering. *Polymers* 2020; 12(9): 1962. doi: 10.3390/polym12091962.
- Radhakrishnan S, Nagarajan S, Belaid H, et al. Fabrication of 3D printed antimicrobial polycaprolactone scaffolds for tissue engineering applications. *Mater Sci Eng C Mater Biol Appl* 2021; 118: 111525. doi: 10.1016/j.msec.2020.111525.
- Park SA, Lee HJ, Kim SY, et al. Three-dimensionally printed polycaprolactone/beta-tricalcium phosphate scaffold was more effective as an rhBMP-2 carrier for new bone formation than polycaprolactone alone. *J Biomed Mater Res A* 2021; 109(6): 840-848.

16. Yang X, Wang Y, Zhou Y, et al. The application of polycaprolactone in three-dimensional printing scaffolds for bone tissue engineering. *Polymers (Basel)* 2021; 13(16): 2754. doi: 10.3390/polym13162754.
17. Mohd Pu'ad NAS, Koshy P, Abdullah HZ, et al. Syntheses of hydroxyapatite from natural sources. *Heliyon* 2019; 5(5): e01588. doi: 10.1016/j.heliyon.2019.e01588.
18. Mohd Zaffarin AS, Ng SF, Ng MH, et al. Nano-hydroxyapatite as a delivery system for promoting bone regeneration *in vivo*: a systematic review. *Nanomaterials (Basel)* 2021; 11(10): 2569. doi: 10.3390/nano11102569.
19. Bal Z, Kaito T, Korkusuz F, et al. Bone regeneration with hydroxyapatite-based biomaterials. *Emergent Mater* 2020; 3(4): 521-544.
20. Ozsagir ZB, Saglam E, Sen Yilmaz B, et al. Injectable platelet-rich fibrin and microneedling for gingival augmentation in thin periodontal phenotype: a randomized controlled clinical trial. *J Clin Periodontol* 2020; 47(4): 489-499.
21. Liu K, Huang Z, Chen Z, et al. Treatment of periodontal intrabony defects using bovine porous bone mineral and guided tissue regeneration with/without platelet-rich fibrin: a randomized controlled clinical trial. *J Periodontol* 2021; 92(11): 1546-1553.
22. Benalcázar Jalkh EB, Tovar N, Arbex L, et al. Effect of leukocyte-platelet-rich fibrin in bone healing around dental implants placed in conventional and wide osteotomy sites: a pre-clinical study. *J Biomed Mater Res B Appl Biomater* 2022; 110(12): 2705-2713.
23. Jia K, You J, Zhu Y, et al. Platelet-rich fibrin as an autologous biomaterial for bone regeneration: mechanisms, applications, optimization. *Front Bioeng Biotechnol* 2024; 12: 1286035. doi: 10.3389/fbioe.2024.1286035.
24. Beiranvand SY, Nourani H, Kazemi Mehrjerdi H. Fabrication of platelet-rich fibrin-coated polycaprolactone/hydroxyapatite (PCL-HA/PRF) 3D printed scaffolds for bone tissue engineering. *Iran J Vet Med* 2022; 16(4): 400-413.
25. Dadgar N, Ghiaseddin A, Irani S, et al. Cartilage tissue engineering using injectable functionalized demineralized bone matrix scaffold with glucosamine in PVA carrier, cultured in microbioreactor prior to study in rabbit model. *Mater Sci Eng C Mater Biol Appl* 2021; 120: 111677. doi: 10.1016/j.msec.2020.111677.
26. Wang X, Zhang Y, Choukroun J, et al. Effects of an injectable platelet-rich fibrin on osteoblast behavior and bone tissue formation in comparison to platelet-rich plasma. *Platelets* 2018; 29(1): 48-55.
27. Mesgarani H, Movafagh J, Nourani H, et al. Treatment of critical-sized calvarial non-union defect *via* collagen-polyglycolic acid scaffold loading with simvastatin in rabbits. *IJVST* 2016; 8(2): 10-99.
28. Liu Y, Wang H, Dou H, et al. Bone regeneration capacities of alveolar bone mesenchymal stem cells sheet in rabbit calvarial bone defect. *J Tissue Eng* 2020; 11: 2041731420930379. Doi: 10.1177/2041731420930379.
29. Aghayan Sh, Asghari A, Mortazavi P, et al. Histomorphometric effects of 2% risedronate gel on calvarial bone defects in rabbits. *J Dent Shiraz Univ Med Sci* 2021; 22(1): 14-20.
30. Musson DS, Gao R, Watson M, et al. Bovine bone particulates containing bone anabolic factors as a potential xenogenic bone graft substitute. *J Orthop Surg Res* 2019; 14(1): 60. doi: 10.1186/s13018-019-1089-x.
31. Emery SE, Brazinski MS, Koka A, et al. The biological and biomechanical effects of irradiation on anterior spinal bone grafts in a canine model. *J Bone Joint Surg Am* 1994; 76(4): 540-548.
32. Wang H, Qi LL, Shema C, et al. Advances in the role and mechanism of fibroblasts in fracture healing. *Front Endocrinol (Lausanne)* 2024; 15: 1350958. doi: 10.3389/fendo.2024.1350958.
33. Meimandi-Parizi A, Oryan A, Sayahi E, et al. Propolis extract a new reinforcement material in improving bone healing: an *in vivo* study. *Int J Surg* 2018; 56: 94-101.
34. Kim HW, Knowles JC, Kim HE. Hydroxyapatite/poly (epsilon -caprolactone) composite coatings on hydroxyapatite porous bone scaffold for drug delivery. *Biomaterials* 2004; 25(7-8): 1279-1287.
35. Calandrelli L, Immirzi B, Malinconico M, et al. Natural and synthetic hydroxyapatite filled PCL: mechanical properties and biocompatibility analysis. *J Bioact Compat* 2004; 19(4): 301-313.
36. Mapara M, Thomas BS, Bhat KM. Rabbit as an animal model for experimental research. *Dent Res J* 2012; 9(1): 111-118.
37. Hämmerle CH, Schmid J, Lang NP, et al. Temporal dynamics of healing in rabbit cranial defects using guided bone regeneration. *J Oral Maxillofac Surg* 1995; 53(2): 167-174.
38. Hwan Jung M, Hun Lee J, Wadhwa P, et al. Bone regeneration in peri-implant defect using autogenous tooth biomaterial enriched with platelet-rich fibrin in animal model. *Appl Sci* 2020; 10(6): 1939. doi: 10.3390/app10061939
39. Kim YK, Kim SG, Byeon JH, et al. Development of a novel bone grafting material using autogenous teeth. *Oral Surg Oral Med Oral Pathol Oral Radiol Endod* 2010; 109(4): 496-503.
40. Faot F, Deprez S, Vandamme K, et al. The effect of L-PRF membranes on bone healing in rabbit tibiae bone defects: micro-CT and biomarker results. *Sci Rep* 2017; 7: 46452. doi: 10.1038/srep46452.
41. Lee JW, Kim SG, Kim JY, et al. Restoration of a peri-

- implant defect by platelet-rich fibrin. *Oral Surg Oral Med Oral Pathol Oral Radiol* 2012; 113(4): 459-463.
42. Lee YK, Wadhwa P, Cai H, et al. Micro-CT and histomorphometric study of bone regeneration effect with autogenous tooth biomaterial enriched with platelet-rich fibrin in an animal model. *Scanning* 2021; 2021: 6656791. doi: 10.1155/2021/6656791.
43. Jung RE, Schmoekel HG, Zwahlen R, et al. Platelet-rich plasma and fibrin as delivery systems for recombinant human bone morphogenetic protein-2. *Clin Oral Implants Res* 2005; 16: 676-682.
44. Chen MC, Chiu HC, Kuo PJ, et al. Bone formation with functionalized 3D printed poly- ϵ -caprolactone scaffold with plasma-rich-fibrin implanted in critical-sized calvaria defect of rat. *J Dent Sci* 2021; 16(4): 1214-1221.
45. Pavlovic V, Ciric M, Jovanovic V, et al. Platelet-rich fibrin: basics of biological actions and protocol modifications. *Open Med (Wars)* 2021; 16(1): 446-454.
46. Filipowska J, Tomaszewski KA, Niedźwiedzki Ł, et al. The role of vasculature in bone development, regeneration and proper systemic functioning. *Angiogenesis* 2017; 20(3): 291-302.
47. Yu H, VandeVord PJ, Mao L, et al. Improved tissue-engineered bone regeneration by endothelial cell mediated vascularization. *Biomaterials* 2009; 30(4): 508-517.
48. Midy V, Hollande E, Rey C, et al. Adsorption of vascular endothelial growth factor to two different apatitic materials and its release. *J Mater Sci Mater Med* 2001; 12(4): 293-298.
49. Pezzatini S, Solito R, Morbidelli L, et al. The effect of hydroxyapatite nanocrystals on microvascular endothelial cell viability and functions. *J Biomed Mater Res A* 2006; 76(3): 656-663.
50. Stayton PS, Drobny GP, Shaw WJ, et al. Molecular recognition at the protein-hydroxyapatite interface. *Crit Rev Oral Biol Med* 2003; 14(5): 370-376.